Continuous diffraction patterns from circular arrays of carbon nanotubes

Butt, Haider; Butler, Tim; Montelongo, Yunuen; Rajesekharan, Ranjith; Wilkinson, Timothy D.; Amaratunga, Gehan A J; Butt, Haider

DOI:
10.1063/1.4770503

Continuous diffraction patterns from circular arrays of carbon nanotubes

Haider Butt, Tim Butler, Yunuen Montelongo, Ranjith Rajesekharan, Timothy D. Wilkinson, and Gehan A. J. Amaratunga

Citation: Applied Physics Letters **101**, 251102 (2012); doi: 10.1063/1.4770503
View online: http://dx.doi.org/10.1063/1.4770503
View Table of Contents: http://scitation.aip.org/content/aip/journal/apl/101/25?ver=pdfcov
Published by the AIP Publishing

APPLIED PHYSICS LETTERS **101**, 251102 (2012)

Continuous diffraction patterns from circular arrays of carbon nanotubes

Haider Butt,[1,a)] Tim Butler,[1] Yunuen Montelongo,[1] Ranjith Rajesekharan,[2]
Timothy D. Wilkinson,[1] and Gehan A. J. Amaratunga[1,3]
[1]*Electrical Engineering Division, Department of Engineering, University of Cambridge, Cambridge CB3 0FA, United Kingdom*
[2]*School of Physics, University of Melbourne, Victoria 3010, Australia*
[3]*Sri Lanka Institute of Nanotechnology (SLINTEC), Lot 14, Zone A, EPZ, Biyagama, Sri Lanka*

(Received 23 July 2012; accepted 4 September 2012; published online 17 December 2012)

We report the remarkable diffraction effects produced from circular patterned arrays of multiwalled carbon nanotubes (MWCNTs). Highly ordered circular arrays of multiwalled carbon nanotubes (with inter-nanotube spacings of 633 nm) display optical dispersion effects similar to compact discs. These arrays display remarkable diffraction patterns in the far field which are spatially continuous. High quality diffraction patterns were obtained experimentally which are in excellent agreement with the theoretical calculations. The achieved continuous diffraction patterns pave the way towards the utilization of engineered carbon nanotube arrays in applications like three dimensional holograms. © *2012 American Institute of Physics*. [http://dx.doi.org/10.1063/1.4770503]

Optical properties of multiwalled carbon nanotubes (MWCNTs) have been thoroughly studied in recent years, and myriad interesting applications have been reported including optical antennas,[1] photonic crystals,[2,3] solar cells,[4] and metamaterials.[5,6] Due to the advancements in nanofabrication techniques, highly controlled growth of carbon nanotubes (with required dimensions) at predefined spatial locations is now possible. CNTs arrays can be fabricated with spacings that are comparable to the wavelengths of visible light, giving rise to interesting optical effects like diffraction.[7] Kempa *et al.*,[2] reported the diffraction related color changing effects from ordered honeycomb arrays of carbon nanotubes. In response to the incident light, these arrays produced diffraction patterns consisting of hexagonally ordered discrete spots. We however report the remarkable spatially continuous diffraction patterns produced from circular patterned arrays of carbon nanotubes. In these arrays, each nanotube acts as a nanoscale diffractive site while displaying a strong optical interaction. On the other hand, the nanotube array as a whole acts as an Fraunhofer hologram,[8] generating a far field intensity profile across the diffracted light. Our Fourier analysis predicted that in response to an incident light, the circular MWCNT array produces a spatially continuous circular diffraction patterns.

Here, we first present the fabrication of highly ordered circular array of MWCNTs. Due to the high degree of ordering, the array displayed very notable optical dispersion effects similar to those of a compact disc. High quality far filed diffraction patterns were obtained experimentally by shining a laser on the array. The patterns were compared with simulated results and an excellent agreement was observed. The presented continuous diffraction patterns pave the way towards the potential usage of MWCNTs as nanoscale diffractive elements[9] (pixels) for applications like three dimensional (3D) holographics.

[a)]Telephone: 44-1223-748353. Fax: 44-1223-748310. Email: hb319@cam.ac.uk.

The large area growth of vertically aligned arrays of multiwalled carbon nanotubes, at predefined locations with controlled dimensions, is possible through the standardized processes of electron beam lithography and plasma-enhanced chemical vapor deposition (PECVD).[10,11] This makes MWCNTs potentially very promising subwavelength nanostructures for producing optical applications requiring nanoscale diffractive elements.[6] Hence, we utilized the circular arrays of MWCNTs for studying the prospective continuous diffraction patterns.

The MWCNT array was fabricated on a 10×10 mm silicon (Si) substrate which was first cleaned and then spin-coated with a 150 nm layer of poly methyl methacrylate (PMMA). The sample was then patterned using a NanoBeam electron beam lithography system and developed for 70 s in a solution of MIBK (methyl isobutyl ketone):IPA (isopropyl alcohol) at a ratio of 1:2. A 5 nm barrier layer of ITO followed by 15 nm of Ni catalyst was sputtered in an argon atmosphere at a pressure of 3.5 mbars. Subsequently, lift-off was carried out in acetone, leaving the desired pattern of catalyst dots. The nanotubes were grown in a NanoInstruments "Black Magic" PECVD system with acetylene as the feedstock gas and ammonia as the etchant. The plasma was maintained at a voltage of 650 V and a current of 60 mA. A growth time of 25 min at a pressure of $\sim$3 mbars yielded a 2.5 mm^2 circular MWCNT array with a tube length of approximately 1800 nm. Scanning electron microscopy (SEM) image of the fabricated CNT array is shown in Figure 1(a), with a magnified view in Figure 1(b). A highly ordered array of vertically aligned MWCNTs was obtained with approximate inter-nanotube spacing of 633 nm.

After growth, the circular MWCNT array appeared colorful and displayed remarkable optical dispersion effects (Figures 1(c)–1(f)). The dispersion effects resembled to those displayed by the compact disc, where a circular pattern of grooves causes beam splitting of the incident white light and all colors of the spectra can be perceived. The beam splitting effects were highly angle dependent due to the 3D structure of MWCNTs and the varying effective inter-nanotube spacing

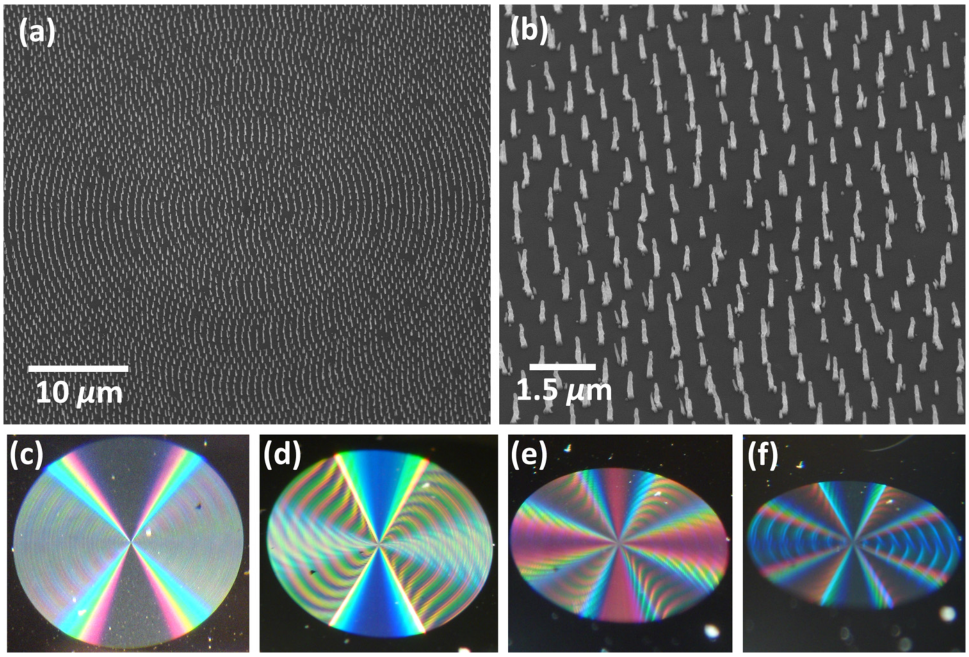

FIG. 1. (a) SEM image of a circular patterned array of multiwalled carbon nanotubes. (b) The same with higher magnification. The compact disc like visible dispersion effects produced by the circular MWCNT array, when viewed from angles of (c) 10°, (d) 30°, (e) 55°, and (f) 70° with the vertical.

offered to the incident light at different angles.[12] The images in Figures 1(c)–1(f) show the dispersion effects observed from an optical microscope at different viewing angles.

To analytically predict the diffraction patterns produced by the MWCNT array, the concept of Fourier optics was utilised.[8] The circular array of nanotubes acts like a hologram (set of apertures) towards the reflected electromagnetic waves, producing a diffraction pattern (replay field) in the far field described by the process of Fraunhofer diffraction. The resultant diffraction pattern can be accurately calculated by taking the fast Fourier transform (FFT) of the holograms. However, in contrast to the conventional two dimensional (2D) holograms, MWCNT arrays have a 3D structure that causes a perturbation of the electromagnetic field in an anisotropic manner. Therefore, the diffraction produced by a light beam shining on an array of CNTs is expected to be dependent on the angle of incidence.[12,13]

Figure 2 shows two different simulations of the far field diffraction patterns produced by the circular pattern of MWCNTs. Figure 2(b) represents a computed diffraction pattern for a normally incident beam reflected from the sample. In this case, the diffractive elements (MWCNTs) are considered as 2D Dirac delta array which means that the nanotube does not have any intrinsic 3D shape associated in

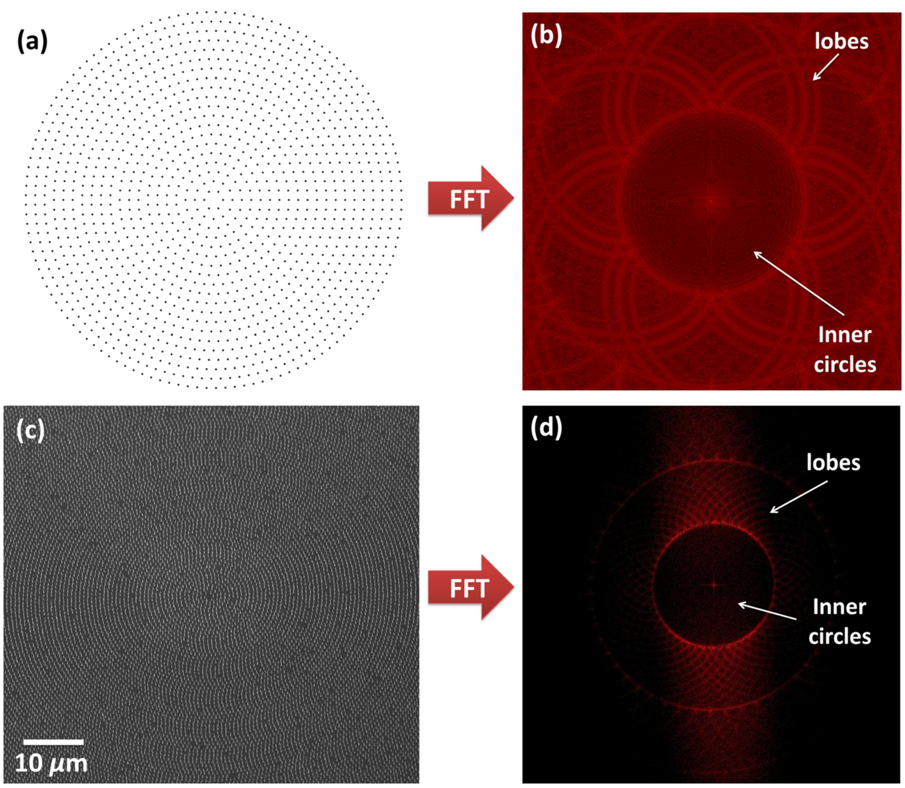

FIG. 2. (a) 2D circular array of MWCNTs. (b) Cropped image of a 2D Fourier transform of the nanotube array producing a continuous diffraction pattern consisting of concentric circles and lobes. (c) SEM image of MWCNT array taken at 30° from the vertical. (d) 2D FFT of the SEM image produces a diffraction pattern with an intensity envelope dictated by the nanotube shape.

the simulation. According to the Fourier theory, the shape of the CNT (the unit diffractive element) has an impact on the overall envelope of the far field pattern. Due to the normal incidence, this impact was minimal in this simulation. The computed diffraction pattern shown in Figure 2(b) consisted for several continuous features, most prominent of which were a series of concentric circles and lobes at the edges of the major circle. The diffraction pattern presents a high continuity and distinction from the conventional patterns consisting of discrete spots and orders.

To study the angular change in the diffraction pattern, an additional pattern was simulated by performing a 2D FFT of the SEM image of the CNT array. The SEM image (Figure 2(c)) was taken at an angle of 30° from the vertical. In this case, the simulation considered the MWCNT shape which dictates an intensity envelop over the computed diffraction pattern (Figure 2(d)), making it dark at the edges. The computed diffraction pattern result also shows that with increase in the number of MWCNTs, the lobes at the edge of the main circle decrease in size and increase in number. The inner concentric circles become finer within the main circle and are not visible in Figure 2(d) due to the large image. Both the simulations highlight different features of the far field diffraction patterns generated by the circular MWCNT array.

The diffraction pattern from the circular MWCNT array was experimentally characterized using an experimental setup attached to a goniometer. The schematic diagram of the setup is shown in Figure 3. The setup consisted of a He-Ne laser as an illumination source for the sample placed on a goniometer. The sample was illuminated from an incidence angle of near 40°. As the spacing between the nanotubes was of the order of incident wavelength (633 nm), therefore, the first order diffracted light was expected at wide angles of around 60° from the zero order (non-diffracted light). Capturing the complete diffraction pattern (view of 180°) was challenging, therefore, two separate screens were placed at different positions to capture different crucial parts of the pattern. The screens were placed at a distance of around 30 cm from the sample. The intensity patterns of light on the screens were captured with a digital single-lens reflex (DSLR) camera. The zero order was blocked to avoid camera saturation.

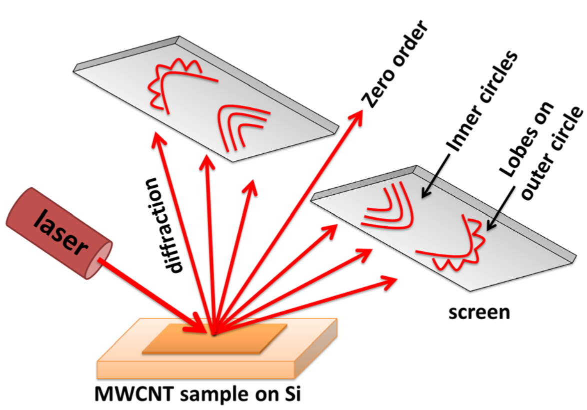

FIG. 3. The schematic diagram of the experimental setup used to characterize the diffraction patterns.

Figure 4 shows the pictures obtained for the continuous diffraction patterns which are in excellent agreement with the simulated results. The pattern consisted of weak inner concentric circles surrounding the zero order (non diffracted or reflected light) and a strong outer circle surrounded by the mesh-like lobes. Figures 4(a) and 4(b) show the inner concentric circles which were very weak in intensity as compared to the outer major circle shown in Figure 4(c). This is in agreement with the simulated results in Figures 2(b) and 2(d) where it can be observed that the inner circles have a lower intensity as compared to the outer circle. The inner circles around the zero order were captured by having a longer camera exposure time. The outer circle was prominent due to high intensity and surrounded by a mesh-like pattern of lobes. As predicted by the simulations results, the lobes were small sized and vast in number due to the interaction of laser with lots of MWCNTs. The diffraction efficiency of the sample was calculated using the equation, diffraction efficiency $= \sum I/I_o$, where I is the sum of intensity in all of the diffracted light and I_o is the intensity of the incident beam.[14] Incident light was diffracted at large angles and its intensity could not be directly measured. I_o was measured directly from the laser while the intensity of zero order was measured as I_z. Hence, $\sum I$ was calculated as $I_o - I_z$. The average efficiency of near 60% (including absorption from nanotubes) was measured at the incident angle of 40°.

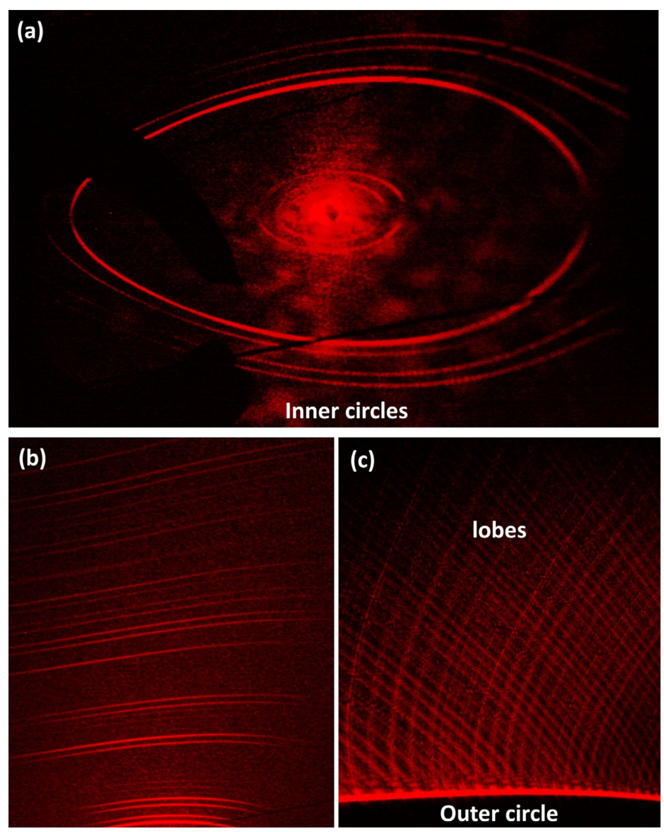

FIG. 4. Captured diffraction patterns produced by the circular MWCNT array. (a) The inner concentric circles surrounding the reflection spot (zero order). (b) The inner circles captured from a different angle with a longer camera exposure time. (c) An edge of the outer major circle (having higher intensity) surrounded by a mesh of lobes.

The diffraction efficiency shows polarization and incident angle dependence as previously reported in Refs. 13 and 15.

Two important characteristics of the experimental results (Figure 4) are the stretching of the diffraction pattern and the darkening of its lateral edges. The stretching of the pattern can be noticed clearly in Figure 4(a) where the circles are expanded in the horizontal direction. The lateral darkening of the whole pattern can also be observed in Figure 4(b), where the pattern disappears on both sides of the profile as predicted by the second simulation in Figure 2(d). These effects are dependent on the inclination of the sample. First, the stretching of the diffraction pattern occurs due to the shrinkage of the nanotube array in the same direction. This effect also occurs in conventional 2D Fraunhofer holograms when tilted.

Second, the lateral darkening of the pattern occurs because the shape of MWCNT changes at different angles. The high aspect ratio of MWCNTs changes rapidly with angle. While the nanotubes appear as spots at normal incidence, their 2D projection can change to a line at wider angles. The increment in size of the diffractive element produces shrinkage of the diffraction pattern envelope in the same direction.

In conclusion, we have demonstrated strong continuous diffraction patterns produced from circular arrays of vertically aligned multiwalled carbon nanotubes. Carbon nanotubes behave as highly diffractive optical elements and their circular ordered arrays cause the diffraction of light into continuous circular and lobes like patterns in far field. The experiment measured diffraction patterns that were in close agreement with the simulated results. Due to the 3D structure of carbon nanotubes, changes in the intensity profiles are observed with the change in incidence angle. The results show that engineered carbon nanotube arrays can be used as anisotropic diffractive media for 3D spatial light modulators and specifically as holograms.

This work was also partly funded under the Nokia-Cambridge Strategic Partnership in Nanoscience and Nanotechnology (Energy Programme). The authors thank Ananta Palani and Qing Dai for the fruitful discussions.

[1]K. Kempa, J. Rybczynski, Z. Huang, K. Gregorczyk, A. Vidan, B. Kimball, J. Carlson, G. Benham, Y. Wang, A. Herczynski, and Z. F. Ren, Adv. Mater. **19**, 421–426 (2007).
[2]K. Kempa, B. Kimball, J. Rybczynski, Z. P. Huang, P. F. Wu, D. Steeves, M. Sennett, M. Giersig, D. V. G. L. N. Rao, D. L. Carnahan, D. Z. Wang, J. Y. Lao, W. Z. Li, and Z. F. Ren, Nano Lett. **3**, 13–18 (2003).
[3]E. Lidorikis and A. C. Ferrari, ACS Nano **3**, 1238–1248 (2009).
[4]H. Zhou, A. Colli, A. Ahnood, Y. Yang, N. Rupesinghe, T. Butler, I. Haneef, P. Hiralal, A. Nathan, and G. A. J. Amaratunga, Adv. Mater. **21**, 3919–3923 (2009).
[5]H. Butt, Q. Dai, P. Farah, T. Butler, T. D. Wilkinson, J. J. Baumberg, and G. A. J. Amaratunga, Appl. Phys. Lett. **97**, 163102–3 (2010).
[6]H. Butt, Q. Dai, R. Rajesekharan, T. D. Wilkinson, and G. A. J. Amaratunga, ACS Nano **5**, 9138–9143 (2011).
[7]J. Rybczynski, K. Kempa, Y. Wang, Z. F. Ren, J. B. Carlson, B. R. Kimball, and G. Benham, Appl. Phys. Lett. **88**, 203122 (2006).
[8]J. W. Goodman, *Introduction to Fourier Optics* (Roberts and Company, 2005).
[9]H. Butt, Y. Montelong, T. Butler, R. Rajesekharan, Q. Dai, S. G. Shiva-Reddy, T. D. Wilkinson, and G. A. J. Amaratunga, Adv. Mater. **24**, OP331–OP336 (2012).
[10]K. B. K. Teo, M. Chhowalla, G. A. J. Amaratunga, W. I. Milne, D. G. Hasko, G. Pirio, P. Legagneux, F. Wyczisk, and D. Pribat, Appl. Phys. Lett. **79**, 1534–1536 (2001).
[11]M. Chhowalla, K. B. K. Teo, C. Ducati, N. L. Rupesinghe, G. A. J. Amaratunga, A. C. Ferrari, D. Roy, J. Robertson, and W. I. Milne, J. Appl. Phys. **90**, 5308–5317 (2001).
[12]K. C. Hsieh, T. Y. Tsai, D. H. Wan, H. L. Chen, and N. H. Tai, Carbon **48**, 1410–1417 (2010).
[13]B. R. Kimball, J. B. Carlson, D. M. Steeves, K. Kempa, Z. Ren, P. Wu, T. Kempa, G. Benham, Y. Wang, W. Li, A. Herczynski, J. Rybczynski, and D. V. Rao, Proc. SPIE **5515**, 223–229 (2004).
[14]M. D. Fayer, Annu. Rev. Phys. Chem. **33**, 63–87 (1982).
[15]B. Kimball, J. B. Carlson, A. Pembroke, K. Kempa, Z. F. Ren, P. Wu, C. Yelleswarapu, T. Kempa, G. Benham, Y. Wang, A. Herczynski, J. Rybczynski, Z. P. Huang, and D. V. G. L. N. Rao, Proc. SPIE **5931**, 59310X (2005).